Benchmark Calculations of Reaction Energies, Barrier Heights, and Transition-State Geometries for Hydrogen Abstraction from Methanol by a Hydrogen Atom

Jingzhi Pu and Donald G. Truhlar*

Department of Chemistry and Supercomputer Institute, University of Minnesota, 207 Pleasant Street S.E., Minneapolis, Minnesota 55455-0431

Received: September 29, 2004; In Final Form: November 18, 2004

We report benchmark calculations of reaction energies, barrier heights, and transition-state geometries for the reaction of CH_3OH with H to produce CH_2OH and H_2. Highly accurate composite methods, such as CBS, G2, G3S, G3X, G3SX, and multi-coefficient correlation methods (MCCMs), are used to calibrate lower-cost methods. We also performed single-level CCSD(T) calculations extrapolated to the infinite-basis limit on the basis of aug-cc-pV*X*Z ($X = 3, 4$) correlation consistent basis sets. The benchmark high-level calculations give consensus values of the forward reaction barrier height and the reaction energy of 9.7 kcal/mol and −6.4 kcal/mol, respectively. To evaluate the accuracy of cost-efficient methods that are potentially useful for dynamics studies of the title reaction, we further include the results obtained by hybrid density functional theory methods and hybrid meta density functional theory methods that have recently been designed for chemical kinetics. Results obtained by popular semiempirical methods are also given for comparison. On the basis of the benchmark gas-phase results, we suggest MC-QCISD/3, MC3BB, and BB1K as reasonably accurate and affordable electronic structure methods for calculating dynamics for the title reaction.

1. Introduction

One of the most important steps in calculating reaction rate constants by variational transition-state theory[1−5] (VTST) is to obtain accurate approximations to the stationary points on reliable potential energy surface (PES). The past several decades have seen tremendous progress in developing accurate and affordable electronic structure methods to provide potential energy information for various size systems.[6−10] However, the large majority of these methods are designed for stable chemical species, that is, for energy minima on PESs. Very recently, though, reaction barrier heights and transition-state properties were introduced as criteria for developing methods that are particularly useful for chemical kinetics.[11−18] With the availability of "accurate for dynamics" PES methods, reliable calculations of reaction rate constants become feasible for systems with more than three or four atoms.

Methanol has been suggested as a potential substitute for fossil fuel since its combustion produces significantly less air pollutants than that of gasoline.[19] Under fuel-rich conditions, a large fraction of methanol is consumed by the reaction with atomic hydrogen.[20] Undoubtedly, the kinetics of methanol reacting with hydrogen plays an important role in combustion. The reaction of methanol with H also provides a prototype for DNA damage that occurs under ionizing rediation, where the hydrogen abstraction step from deoxyribose is believed to lead to a broken DNA strand and ultimately to cell death.[21]

Because of its general importance in combustion, atmospheric chemistry, and biological systems, the title reaction has been subjected to a large number of experimental studies and theoretical calculations. A gas-phase rate expression has been suggested by Tsang in a chemical kinetics database.[22] Significant kinetic isotope effects (KIEs) have been reported by several groups.[23−25] In particular, the KIEs for a deuterium atom attacking methanol have been measured both in the gas phase[24] and in aqueous solution.[25] To elucidate the solvation effect on the reaction dynamics, Chuang et al. performed rate constant calculations[26] for $CH_3OH + H$ employing variational transition-state theory with multidimensional tunneling (VTST/MT) on the basis of a potential energy surface obtained by a linear combination of Hartree−Fock[27] (HF) and Austin model 1[28] (AM1). In their solution-phase calculations, the free energy of solvation was obtained by the SM5.42 solvation model.[29] By using a collective solvent coordinate, the nonequlibrium solvation effect for this reaction was also addressed.[30] Although sophisticated dynamics models have been applied in these calculations, the quantitative results are still largly determined by the quality of the potential energy surface. The potential energy surface for this system has been characterized by various other levels of theory,[26,31−33] but unfortunately the various theoretical estimates do not agree with each other within chemical accuracy.

In the current work, we reexamine the reactive barrier height and reaction energy by applying a wide spectrum of electronic structure methods, especially including the recently developed methods that are designed for chemical kinetics. Our first goal is to obtain benchmark values for these two energetic quantities and for the transition-state geometry for the title reaction. On the basis of these reliable consensus results, the uncertainty of the stationary points on the potential energy surface that impedes the reliable reaction rate calculations can be largely removed. Then, the second goal is to identify the least expensive levels of electronic structure theory that give a reasonably accurate barrier height and energy of reaction.

The paper is organized as follows. Section 2 describes methods we used in our calculations. Section 3 presents the energetic and geometric results and discussion. A brief summary of our calculations is given in Section 4 as concluding remarks.

* Corresponding author.

10.1021/jp045574v CCC: $30.25
Published on Web 01/19/2005

2. Computational Details

We calculated the zero-point-exclusive energy of reaction and the classical barrier heights for both the forward and reverse reactions of $CH_3OH + H \rightarrow CH_2OH + H_2$. These energies are either calculated using single-point methods or by full geometry optimization. We denote the single-point energy calculations as X//Y, where a single- point energy calculation at level X is carried out for the geometry optimized at a lower level Y. If X is identical to Y, we simply denote the calculation as X. The methods used for geometry optimization include the HF method;[27] Møller−Plesset second-order (MP2) perturbation theory;[34] two hybrid density functional methods: MPW1K[11] and B3LYP;[35] four hybrid meta density functional methods: B1B95,[15,36] BB1K,[15] MPW1B95,[17] and MPWB1K;[17] five multi-coefficient correlation methods (MCCMs): multi-coefficient Gaussian-2, version 3 (MCG2/3),[12a,14] multi-coefficient Gaussian-3, version 3 (MCG3/3),[12bc,14] and multi-coefficient quadratic configuration interaction with single and double excitations, version 3 (MC-QCISD/3),[12,13] the scaling all correlation method, version 3 (SAC/3);[12,37] and two doubly hybrid density function theory (DHDFT) methods: MC3BB and MC3MPW.[16] For single-point calculations, we have used the coupled cluster method with single, double, and noniterative triple excitations CCSD(T),[38] Gaussian-3 based on scaling[39] (G3S), reduced-order extended G3S[40] [G3SX(MP3)], and four available complete basis set (CBS) models, namely, CBS-APNO,[41] CBS-QB3,[42,43] CBS-Q,[42] and CBS-4M.[43] The basis sets employed for single-level ab initio methods and DFT calculations are the 6-31G(d),[44] 6-31+G(d,p),[44] MIDI!,[45] and MG3S[46a] basis sets. For systems containing only elements no heavier than F, such as in the present study, the MG3S basis set is identical to 6-311+G(2df,2p), in which the diffuse function on hydrogens has been removed from the 6-311++G(2df,2p) basis set.[46b]

The radical species have doublet electronic states and were treated with the unrestricted HF (UHF) method[27b] and unrestricted correlated methods. All single-point calculations were preformed using the GAUSSIAN03 program.[47] The MCCM calculations were performed with the MULTILEVEL 4.0 program.[48] The spin−orbit contribution to the energy is zero for the present systems.[49] The SAC/3, MC-QCISD/3, and MCG3/3 calculations were performed with version 3s coefficients.[14]

The CCSD(T) calculations are carried out using MOLPRO 2002.6.[50] We employ the extrapolation scheme proposed by Helgaker[51a] and used by Csaszar et al.[51b] to obtain the infinite basis-set limit of CCSD(T)/aug-cc-pV*X*Z:

$$E(X) = E_\infty + \frac{b}{X^3} \quad (1)$$

where X represents the number of primitive functions in the most diffuse contracted functions of the split valence basis set (in the current calculation $X = 3$ for valence triple-ζ and 4 for valence quadruple-ζ); $E(X)$ is the energy obtained with a given X, that is, the CCSD(T)/aug-cc-PV*X*Z energy; E_∞ denotes the extrapolated energy corresponding to extrapolated to an infinite basis-set limit; and b is a fitting parameter.

We also perform calculations by using semiempirical molecular orbital theories based on the neglect of differential overlap (NDO) approximation. The NDO methods tested in the present study include AM1[28] and parametrized model 3 (PM3)[52] as implemented in the MOPAC 5.010MN program[53] (the parameters are the same as in MOPAC 5 and MOPAC 6), modified symmetrically orthogonal intermediate neglect of differential overlap (MSINDO)[54] as implemented in MSINDO 2.6,[55] and two pairwise distance directed Gaussian (PDDG) methods,[56] namely, PDDG/PM3 and PM3/MNDO, as implemented in a modified MOPAC 6.[57] The AM1, PM3, PDDG/PM3, and PDDG/MNDO methods are based on neglect of diatomic differential overlap (NDDO).[58] MSINDO is based on intermediate neglect of differential overlap (INDO).[59]

3. Results and Discussion

3.1. Energetics. Table 1 gives the reaction barrier heights, the reaction energies, and the breaking and forming bond energies obtained at various levels of theory. The bond energy for the breaking bond (C−H) is calculated as the dissociation energy of CH_3OH to CH_2OH and H, and the bond energy for the forming bond (H−H) is calculated as the energy difference of H_2 and two hydrogen atoms. The barrier heights, reaction energies, and bond energies are zero-point exclusive. In Table 1, we group the methods by their asymptotic computational scaling behaviors N^α, where N is the number of atoms and α is in the range of 3−7. (Within each group, methods are listed in an approximate order of descending accuracy for barrier heights of hydrogen atom transfer reaction involving first-row atoms, as largely determined by previous[14−17,60] systematic tests.) Apart from the methods that we investigate in the present work, we also include for comparison in Table 1 selected results of Chuang et al.[26] and some representative data available in the literature. The barrier heights and reaction energy based on the very accurate Weizmann-1[61] (W1) method are obtained from a recently constructed database for parametrizing the BMK[18] density functional. Recommended values of both the forward and reverse barrier heights for the reaction of methanol with H had been suggested[11] on the basis of comparisons to experiment and incorporated in a thermochemistry and thermochemical kinetics database called Database/3,[14] but one of the goals of the present work is to test these values in case the experiments are not accurate. The zero-point-exclusive reaction energy[26] and bond energies for breaking the C−H bond[62] and forming the H−H bond[63] in this reaction have been estimated. One can also derive the reaction energy and these bond energies from accurate atomization energies.[14] We list these previously evaluated data in Table 1 as well, and we will evaluate their accuracy against the benchmark results calculated in the present work.

The N^7 methods represent state-of-the-art techniques for computational thermochemistry. First, the W1 method predicts barrier heights and a reaction energy that are closely consistent with the extrapolated CCSD(T) results, which give a forward barrier height of 9.6 kcal/mol. The G3-type methods give a slightly higher forward barrier height, 9.7−10.0 kcal/mol, than that obtained by the W1 method. The CBS methods tend to underestimated the barrier heights, as we[60c] and Coote et al.[64] found in the studies of hydrogen atom transfer reactions between hydrocarbon radicals. In particular, CBS-APNO gives a forward barrier height as low as 9.1 kcal/mol. Altogether, the N^7 methods listed in Table 1 give an average forward barrier height of 9.7 kcal/mol and an average reverse barrier height of 16.0 kcal/mol. We exclude the CCSD(T)/aug-cc-pVDZ//QCISD/MG3 results in calculating these average values, since the CCSD(T) calculation usually requires a large basis set to obtain reliable energies. Consequently, we suggest that the forward barrier height in Database/3 may be too low (7.3 kcal/mol) for this reaction, although the reaction energy used in Database/3 seems to be reasonably accurate (see below).

Although G3-type methods obtain forward barrier heights that are consistent with each other, they predict different reaction

TABLE 1: Reaction Energies, Barrier Heights, and Bond Energies (in kcal/mol)

method	V_f[a]	V_r[b]	ΔE	D_e(C−H)	D_e(H−H)	ref
			N^7 methods			
W1	9.6	15.7	−6.1	103.5[c]	109.6[c]	18
G3SX//B3LYP/6-31G(2df,p)	9.8	15.9	−6.1	103.7	109.8	p.w.[d]
G3SX(MP3)//B3LYP/6-31G(2df,p)	10.0	16.2	−6.3	103.6	109.9	p.w.
G3X//B3LYP/6-31G(2df,p)	9.7	16.4	−6.7	103.3	110.0	p.w.
Ext-CCSD(T)aug-cc-pV*X*Z ($X = 3, 4$)	9.6	15.8	−6.1	103.5	109.6	p.w.
CCSD(T)/aug-cc-pVQZ//QCISD/MG3	9.6	15.6	−6.0	103.1	109.2	p.w.
G3S//MP2(full)/6-31(d)	9.9	15.7	−5.8	103.8	109.6	p.w.
CCSD(T)/aug-cc-pVTZ//QCISD/MG3	9.6	15.4	−5.9	102.7	108.5	p.w.
CBS-QB3//QCISD/MG3	9.5	16.2	−6.7	104.0	110.7	p.w.
CBS-QB3//B3LYP/6-31G(d)	9.4	16.1	−6.7	104.0	110.7	p.w.
CBS-Q//QCISD/MG3	9.4	16.2	−6.8	103.8	110.6	p.w.
CBS-Q//MP2/6-31G(d)	9.0	15.7	−6.7	103.9	110.5	p.w.
MCG2/3//QCISD/MG3	9.7	16.5	−6.8	104.2	111.0	p.w.
MCG3/3	10.0	16.9	−6.9	104.0	110.9	p.w.
MCG3/3//MC-QCISD/3	10.0	16.9	−6.9	103.9	110.9	p.w.
CBS-APNO//QCISD/6-311G(d,p)	9.1	15.2	−6.1	103.8	109.9	p.w.
CBS-APNO//QCISD/MG3	9.1	15.2	−6.1	103.8	109.9	p.w.
G2//MP2/6-31G(d)	9.0	17.2	−8.2	n.a.[e]	n.a.	29
CCSD(T)/aug-cc-pVDZ//QCISD/MG3	10.4	14.1	−3.7	100.4	104.1	p.w.
			N^6 methods			
MC-QCISD/3	10.3	17.2	−6.8	104.4	111.2	p.w.
CBS-4M//QCISD/MG3	10.4	16.2	−5.8	104.2	110.0	p.w.
CBS-4M//UHF/3-21G(d)	10.7	16.1	−5.4	104.6	110.0	p.w.
QCISD/MG3	11.0	17.5	−6.5	100.9	107.4	p.w.
CCSD/cc-pVDZ	10.8	16.3	−5.5	98.1	103.6	26
QCISD/cc-pVDZ	10.5	16.2	−5.7	97.9	103.6	26
QCISD/6-31G(d)	16.6	18.7	−2.1	95.3	97.4	26
			N^5 methods			
MC3BB	9.8	14.6	−4.7	102.5	107.2	p.w.
MC3MPW	9.5	13.8	−4.3	101.2	105.5	p.w.
SAC/3	14.3	16.2	−1.9	104.2	106.1	p.w.
MP2/cc-pVTZ	14.3	16.2	−1.9	101.7	103.6	26
MP2/cc-pVDZ	14.4	15.4	−1.0	97.3	98.3	26
MP2/6-31+G(d,p)	16.8	18.0	−1.9	104.2	106.1	p.w.
MP2(full)/6-31G(d)	20.2	17.7	2.5	95.2	92.7	p.w.
MP2/6-31G(d)	20.2	17.8	2.4	95.1	92.7	26
			N^4 methods			
BB1K/MG3S	8.7	14.5	−5.7	101.6	107.3	p.w.
BB1K/6-31+G(d,p)	8.4	14.2	−5.8	102.8	108.6	p.w.
MPWB1K/MG3S	8.7	13.9	−5.2	102.0	107.1	p.w.
MPW1K/MG3S	7.9	13.5	−5.6	99.4	104.9	p.w.
MPW1K/6-31+G(d,p)	7.7	13.4	−5.6	100.6	106.2	p.w.
B1B95/MG3S	7.0	13.5	−6.5	101.0	107.6	p.w.
MPW1B95/MG3S	7.1	12.9	−5.8	101.5	107.3	p.w.
B3LYP/cc-pVDZ	2.0	10.6	−8.6	98.8	107.4	26
B3LYP/6-31+G(d,p)	3.2	12.9	−9.7	102.0	111.7	p.w.
B3LYP/6-31G(d)	3.6	11.7	−8.1	101.7	109.8	26
B3PW91/6-31G(d)	5.0	11.2	−6.2	100.7	106.8	26
B3LYP/MIDI!	1.7	11.5	−9.8	97.9	107.7	26
AC-SRP	7.8	12.3	−4.5	101.4	106.0	26
HF||AM1-SRP	7.8	12.8	−5.0	105.6	110.7	26
mPWPW91/6-31+G(d,p)	1.9	9.4	−7.6	99.7	107.3	p.w.
HF/cc-pVTZ	19.8	22.5	−2.7	79.0	81.7	26
HF/cc-pVDZ	20.1	24.2	−4.1	79.6	83.7	26
HF/MIDI!	20.1	22.9	−2.9	77.3	80.1	p.w.
HF/6-31G(d)	21.7	22.9	−1.2	80.6	81.8	26
HF/STO-3G	19.1	30.3	−11.2	104.5	115.7	26
			N^3 methods			
AM1-SRP	4.1	9.0	−4.9	104.4	109.3	26
AM1	−0.4	27.6	−28.0	81.4	109.4	p.w.
PM3	0.2	38.7	−38.6	79.0	117.6	p.w.
MSINDO	23.5	37.7	−14.3	94.4	108.7	p.w.
PDDG/PM3	−4.0	53.6	−57.6	79.3	136.9	p.w.
PDDG/MNDO	2.2	46.3	−44.2	74.2	118.4	p.w.
			Other			
Database/3	7.3	13.8	−6.5	103.0	109.5	14
previous estimate			−5.1	104.4	109.5	26,62,63

[a] Forward barrier height. [b] Reverse barrier height. [c] Calculated at the present work. [d] p.w. denotes present work. [e] n.a. denotes not available.

energies with a maximum deviation of 0.9 kcal. In particular, the G3X method seems to overestimate the magnitude of the reaction exothermicity (−6.7 kcal/mol) compared to the W1 result (−6.1 kcal/mol). The CBS methods are designed for accurate atomization energies and therefore should be very reliable in calculating reaction energies. The highest level of CBS methods, that is, CBS-APNO, gives a reaction energy of −6.1 kcal/mol, in a good agreement with W1 and extrapolated CCSD(T) results. However, the other N^7 versions of CBS methods (CBS-Q and CBS-QB3) predict a reaction energy of

6.7−6.8 kcal/mol, which agrees with MCG2 and MCG3 results very well. On average, the N^7 methods give a reaction energy of −6.4 kcal/mol [again, we exclude the CCSD(T) double-ζ basis set result for the same reason as when we calculate the average barrier heights]. Encouragingly, the reaction energy used in Database/3 which is derived from accurate experiment-based atomization energies agrees well with the average value we obtained here from high-level benchmark calculations.

Next, we use the consensus values of the energetics from the N^7 methods, that is, a forward barrier and reaction energy of 9.7 kcal/mol and −6.4 kcal/mol, respectively, to evaluate the accuracy of more cost-efficient methods. Among the N^6 methods, MC-QCISD/3 can be identified as the best method. It gives a forward barrier height (10.3 kcal/mol) that is only slightly too high, and the reaction energy deviates from our best estimate by less than 0.5 kcal/mol. Selecting the most accurate method that is affordable for dynamics calculation is one of our key goals in the present study. Although MC-QCISD/3 gives satisfactory performance on the barrier heights and reaction energetics, the QCISD component in an MC-QCISD/3 calculation is still computationally formidable for calculating a reaction path over a wide reaction coordinate range, especially if a small gradient step is needed to secure a converged path. Furthermore, expensive Hessian calculations required for vibrational analysis at the QCISD level exacerbate the cost situation for an MC-QCISD/3 potential energy surface.

Promising alternatives are the doubly hybrid DFT methods, MC3BB and MC3MPW, which scale to N^5. The most intriguing feature of these methods is that they introduce an MP2 component into the DFT energies,[16] in the spirit of hybrid DFT, where an HF component is mixed into DFT calculations. Table 1 shows that MC3BB and MC3MPW give almost perfect forward reaction barrier heights and reasonable reaction energies. Interestingly, neither the single-level MP2 calculations nor the scaling all correlation (SAC) method can give qualitative correct energetic results without mixing DFT into the equation. The essential element in the DFT is probably the static correlation contained implicitly in the DFT exchange.

One should be able to make further improvement by the aid of the specific reaction parameters[65] (SRP) introduced into these two MC3 methods. The MP2 components in the two doubly hybrid DFT methods are obtained with a small basis set of 6-31+G(d,p),[16] which makes them very suitable for providing the potential energy in dynamics calculations, since for small systems these methods would be as inexpensive as DFT methods using a large basis sets. An even more appealing choice is to use DFT methods or hybrid DFT methods, which scale as N.[4] In the present work, we test several newly developed hybrid DFT (HDFT) methods that are designed for kinetics, in particular, MPW1K, BB1K, and MPWB1K. First of all, in Table 1, all the HDFT methods parametrized for kinetics are superior to pure DFT methods, such as mPWPW91, or to HDFT methods with a lower percentage of HF exchange, such as B3LYP, for predicting reaction barrier heights. The hybrid meta DFT methods with general parametrizations, such as MPW1B95 and B1B95, make significant improvement over the HDFT methods without a kinetic energy density,[66] in terms of both the barrier heights and the reaction energy for the title reaction. In particular, MPW1B95 and B1B95 both give reaction energies of −6.5 kcal/mol, in good agreement with our consensus value, but they predict barrier heights that are too low compared to accurate methods. The predicted barrier heights are significantly improved to 8.7 kcal/mol in BB1K and MPWB1K by increasing the percentage of HF exchange. Furthermore, BB1K also gives a reasonably good reaction energy of −5.7 kcal/mol.

Although identifying accurate NDDO or INDO methods (which scale as N^3) would be useful for applying them to hydrogen abstraction involving alcohols in biological systems,

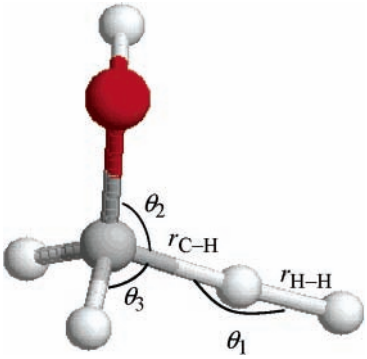

Figure 1. Transition-state geometry for $CH_3OH + H$.

TABLE 2: Key Bond Distances in Transition State (in Å)

method	r_{H-H}[a]	r_{C-H}[b]	sum	ref	MUD[c]
	N^7 methods				
MCG3/3	0.979	1.306	2.286	p.w.[d]	0.000
	N^6 methods				
MC-QCISD/3	0.973	1.309	2.281	p.w.	0.005
QCISD/MG3	0.969	1.316	2.283	p.w.	0.010
QCISD/cc-pVDZ	0.984	1.326	2.310	26	0.013
CCSD/cc-pVDZ	0.980	1.328	2.308	26	0.012
QCISD/6-31G(d)	0.963	1.358	2.321	26	0.034
	N^5 methods				
MC3BB	0.952	1.324	2.276	p.w.	0.022
MC3MPW	0.945	1.328	2.273	p.w.	0.028
SAC/3	0.923	1.340	2.263	p.w.	0.045
MP2/cc-pVTZ	0.928	1.342	2.270	26	0.044
MP2/cc-pVDZ	0.941	1.355	2.296	26	0.044
MP2/6-31+G(d,p)	0.920	1.346	2.266	p.w.	0.050
MP2(full)/6-31G(d)	0.927	1.373	2.301	p.w.	0.059
MP2/6-31G(d)	0.928	1.373	2.301	26	0.059
	N^4 methods				
BB1K/MG3S	0.969	1.311	2.280	p.w.	0.008
BB1K/6-31+G(d,p)	0.968	1.315	2.283	p.w.	0.010
MPWB1K/MG3S	0.965	1.313	2.278	p.w.	0.010
MPW1K/MG3S	0.966	1.311	2.277	p.w.	0.009
MPW1K/6-31+G(d,p)	0.964	1.314	2.279	p.w.	0.011
B1B95/MG3S	0.983	1.306	2.289	p.w.	0.002
MPW1B95/MG3S	0.977	1.309	2.286	p.w.	0.002
B3LYP/cc-pVDZ	1.026	1.299	2.325	26	0.027
B3LYP/6-31+G(d,p)	1.004	1.295	2.299	p.w.	0.018
B3LYP/6-31G(d)	1.011	1.301	2.312	26	0.019
B3PW91/6-31G(d)	1.001	1.308	2.309	26	0.012
B3LYP/MIDI!	1.070	1.261	2.331	26	0.068
AC-SRP	0.971	1.322	2.293	26	0.012
HF||AM1-SRP	0.867	1.277	2.144	26	0.071
mPWPW91/6-31+G(d,p)	1.034	1.280	2.314	p.w.	0.040
HF/cc-pVTZ	0.972	1.346	2.301	26	0.020
HF/cc-pVDZ	0.967	1.334	2.318	26	0.024
HF/MIDI!	0.973	1.343	2.316	p.w.	0.021
HF/6-31G(d)	0.960	1.351	2.311	26	0.032
HF/STO-3G	0.968	1.275	2.243	26	0.021
	N^3 methods				
AM1-SRP	1.104	1.310	2.114	26	0.090
AM1	1.341	1.135	2.467	26	0.267
PM3	1.113	1.458	2.569	p.w.	0.157
MSINDO	1.027	1.239	2.267	p.w.	0.058
PDDG/PM3	2.033	1.108	3.141	p.w.	0.626
PDDG/MNDO	1.153	1.251	2.404	p.w.	0.212

[a] Forming bond distance. [b] Breaking bond distance. [c] MUD is mean unsigned deviation of the r_{H-H} and r_{C-H} distances from the MCG3/3 values. [d] p.w. denotes present work.

TABLE 3: Key Bond Angles in Transition State (in Degrees)

method	θ_1[a]	θ_2[b]	θ_3[c]	MUD[d]
	N^7 methods			
MCG3/3	177.2	110.1	104.1	0.0
	N^6 methods			
MC-QCISD/3	177.1	110.0	104.1	0.1
QCISD/MG3	177.5	110.1	104.0	0.1
	N^5 methods			
MC3BB	178.0	110.4	103.6	0.5
MC3MPW	177.8	110.3	103.6	0.4
SAC/3	177.9	110.5	103.8	0.4
	N^4 methods			
BB1K/MG3S	178.0	110.5	103.5	0.6
BB1K/6-31+G(d,p)	178.4	110.6	103.7	0.7
MPWB1K/MG3S	177.8	110.4	103.5	0.5
MPW1K/MG3S	177.8	110.4	103.4	0.5
MPW1K/6-31+G(d,p)	178.1	110.5	103.6	0.6
B1B95/MG3S	178.7	110.8	103.6	0.9
MPW1B95/MG3S	178.4	110.6	103.6	0.7

[a] C−H−H angle (see Figure 1). [b] O−C−H angle (see Figure 1). [c] H−C−H angle (see Figure 1). [d] MUD is mean unsigned deviation of the three angles from the MCG3/3 values.

where cost-coefficient methods are highly desirable for treating a macromolecular system that usually contains thousands of atoms, the last section of Table 1 shows that no popular generally parametrized semiempirical method is able to give barrier height or reaction energy accurate within 7 kcal/mol for the CH_3OH + H reaction. The specially parametrized AM1-SRP method is more accurate but suffers from having been parametrized to apparently unreliable experimental data.

3.2. Transition-State Geometry. Figure 1 shows the transition-state structure for the reaction of CH_3OH with H, where one of the hydrogen atoms at the gauche position to the hydroxyl group is being abstracted.[26] Table 2 gives the key bond distances at the transition state optimized at various levels of theory and the sum of these distances (also called the perpendicular looseness). All calculations in Table 2 are from the present work. Since the highest-level method at which we fully optimized the transition-state geometry is MCG3/3, we use this geometry as a benchmark to evaluate the performance of other methods. Mean unsigned deviations (MUDs) of the breaking and forming bond distances from the MCG3 results are also tabulated in Table 2 for this purpose. In methods that scale to N^6, MC-QCISD/3 and QCISD/MG3 predict values of these key bond distances that agree well with the results obtained by MCG3/3. The MUDs for MC-QCISD/3 and QCISD/MG3 are 0.005 Å and 0.010 Å, respectively. The small error of the QCISD/MG3 geometry indicates that the geometry we used for high-level double-slash calculations should be sufficiently accurate. It is encouraging that the two MC3 methods perform best in predicting transition-state geometries among all N^5 methods in the present study. In particular, the MC3BB and MC3MPW give MUEs of 0.022 Å and 0.028 Å, respectively. Without the aid of a hybrid DFT or a hybrid meta DFT component, SAC/3 only performs about as well as the single-level MP2 calculations, where MUDs are 0.04−0.06 Å.

The N^4 methods represent promising candidates for dynamics calculations. Among these methods, both the hybrid DFT and hybrid meta DFT methods parametrized for kinetics, that is, MPW1B1K, BB1K, and MPW1K, give small errors comparable to N^6 methods such as MC-QCISD/3 and QCISD/MG3. Although the methods with a general parametrization can perform even better in terms of the transition-state geometry (for example, B1B95/MG3 gives an MUD of only 0.002 Å compared to an MUD of 0.008 Å given by BB1K/MG3), the generally parametrized methods are less promising for kinetic calculations since they usually tend to underestimate the reaction barrier heights.

Table 3 lists the bond angles at the transition state optimized for the most accurate methods recommended by this paper, namely, MCG3/3, MC-QCISD/3, MC3BB, and BB1K. The results of QCISD/MG3, SAC/3, and several hybrid DFT and hybrid meta DFT are also included in Table 3 for comparison. MC-QCISD/3 and QCISD/MG3 are able to predict these key angles in a good agreement with the MCG3/3 results. This is consistent with the conclusion that we draw from the transition-state bond distances. Again, the MC3 and hybrid (meta) DFT methods give very accurate angles for the transition state with small MUDs less than 1 degree.

4. Concluding Remarks

In this article, we have reported benchmark calculations for the classical barrier height, reaction energy, and transition-state geometry of the reaction of hydrogen abstraction from methanol by a hydrogen atom. We obtained a consensus value of the forward reaction barrier height of 9.7 kcal/mol and the reaction energy of −6.4 kca/mol. On the basis of the benchmark results, we identified three reasonably accurate and affordable methods that are most suitable for further dynamics calculations, in particular, MC-QCISD/3, MC3BB, and BB1K. Our results also show that these highly recommended methods are able to predict very accurate transition-state geometries for the title reaction, with MUDs less than or equal to 0.02 Å and 0.7 degree, for bond distances and bond angles, respectively.

Acknowledgment. This work was supported in by the U.S. Department of Energy, Office of Basic Energy Sciences.

References and Notes

(1) Garrett, B. C.; Truhlar, D. G. *J. Chem. Phys.* **1984**, *81*, 309.
(2) Truhlar, D. G.; Isaacson, A. D.; Garrett, B. C. In *Theory of Chemical Reaction Dynamics*; Baer, M., Ed.; CRC Press: Boca Raton, FL, 1985; Vol. 4, p 65.
(3) Kreevoy, M. M.; Truhlar, D. G. In *Investigation of Rates and Mechanisms of Reactions*; Bernasconi, C. F., Ed.; John Wiley & Sons: New York, 1986; Vol. 6, p 13.
(4) Tucker, S. C.; Truhlar, D. G. In *New Theoretical Concepts Understanding Organic Reactions*; J. Bertran, I. G. C., Ed.; Kluwer Academic Publishers: Dordrecht, The Netherlands, 1989; Vol. 267, p 291.
(5) Truhlar, D. G.; Garrett, B. C.; Klippenstein, S. J. *J. Phys. Chem.* **1996**, *100*, 12771. Chuang, Y.-Y.; Corchado, J. C.; Truhlar, D. G. *J. Phys. Chem. A* **1999**, *103*, 1140.
(6) Hehre, W. J.; Radom, L.; Schleyer, P. v.R. Pople, J. A. *Ab Initio Molecular Orbital Theory*; John Wiley & Sons: New York, 1986.
(7) Kohn, W.; Becke, A. D.; Parr, R. G. *J. Phys. Chem.* **1996**, *100*, 12974.
(8) *Combined Quantum Mechanical and Molecular Mechanical Methods*; Gao, J., Thompson, M., Eds.; ACS Symposium Series 712; American Chemical Society: Washington, DC, 1998.
(9) Thiel, W. In *Modern Methods and Algorithms of Quantum Chemistry*, 2nd ed.; Grotendorst, J., Ed.; NIC series, Vol. 3; John von Neumann Institute for Computing: Jülich, Germany, 2000; p 261.
(10) Staszewska, G.; Staszewski, P.; Schultz, N. E.; Truhlar, D. G. *Phys. Rev. B*, in press.
(11) Lynch, B. J.; Fast, P. L.; Harris, M.; Truhlar, D. G. *J. Phys. Chem. A* **2000**, *104*, 4811.
(12) (a) Fast, P. L.; Sanchez, M. L.; Corchado, J. C.; Truhlar, D. G. *J. Chem. Phys.* **1999**, *110*, 11679. (b) Tratz, C. M.; Fast, P. L.; Truhlar, D. G. *PhysChemComm* **1999**, *2*, Article 14. (c) Fast, P. L.; Sanchez, M. L.; Truhlar, D. G. *Chem. Phys. Lett.* **1999**, *306*, 407.
(13) Fast, P. L.; Truhlar, D. G. *J. Phys. Chem. A* **2000**, *104*, 6111.
(14) Lynch, B. J.; Truhlar, D. G. *J. Phys. Chem. A* **2003**, *107*, 3898.
(15) Zhao, Y.; Lynch, B. J.; Truhlar, D. G. *J. Phys. Chem. A* **2004**, *108*, 2715.
(16) Zhao, Y.; Lynch, B. J.; Truhlar, D. G. *J. Phys. Chem. A* **2004**, *108*, 4786.

(17) Zhao, Y.; Truhlar, D. G. *J. Phys. Chem. A* **2004**, *108*, 6908.
(18) Boese, A. D.; Martin, J. M. L. *J. Chem. Phys.* **2004**, *121*, 3405.
(19) (a) Aronowitz, D.; Naegeli, D. W.; Glassman, I. *J. Phys. Chem.* **1977**, *81*, 2555. (b) Norton, T. S.; Dryer, F. L. *Int. J. Chem. Kinet.* **1990**, *22*, 219. (c) Marshall, E. *Science* **1989**, *246*, 1999. (d) Morton, L.; Hunter, N.; Gesser, H. *Chem. Ind.* **1990**, 457.
(20) Grotheer, H. H.; Kelm, S.; Driver, H. S. T.; Hutcheon, R. J.; Lockett, R. D.; Robertson, G. N. *Ber. Bunsen-Ges. Phys. Chem.* **1992**, *96*, 1360.
(21) Pardo, L.; Banfelder, J. R.; Osman, R. *J. Am. Chem. Soc.* **1992**, *114*, 2382.
(22) Tsang, W. *J. Phys. Chem. Ref. Data* **1987**, *16*, 471.
(23) (a) Campion, A.; Williams, F. *J. Am. Chem. Soc.* **1972**, *94*, 7633. (b) Hudson, R. L.; Shiotani, M.; Williams, F. *Chem. Phys. Lett.* **1977**, *48*, 193. (c) Doba, T.; Ingold, K. U.; Siebrand, W.; Wildman, T. A. *Faraday Discuss. Chem. Soc.* **1984**, *78*, 175. (d) Doba, T.; Ingold, K. U.; Siebrand, W.; Wildman, T. A. *J. Phys. Chem.* **1984**, *88*, 3165.
(24) Meagher, J. F.; Kim, P.; Lee, J. H.; Timmons, R. B. *J. Phys. Chem.* **1974**, *78*, 2650.
(25) Lossack, A. M.; Roduner, E.; Bartels, D. M. *J. Phys. Chem. A* **1998**, *102*, 7462.
(26) Chuang, Y.-Y.; Radhakrishnan, M. L.; Fast, P. L.; Cramer, C. J.; Truhlar, D. G. *J. Phys. Chem. A* **1999**, *103*, 4893.
(27) (a) Roothaan, C. C. J. *Rev. Mod. Phys.* **1951**, *23*, 69. (b) Pople, J. A.; Nesbet, R. K. *J. Chem. Phys.* **1954**, *22*, 571.
(28) (a) Dewar, M. J. S.; Zoebisch, E. G.; Healy, E. F.; Stewart, J. J. P. *J. Am. Chem. Soc.* **1985**, *107*, 3902. (b) Holder, A. J.; Dennington, R. D.; Jie, C.; Yu, G. *Tetrahedron* **1994**, *50*, 627. (c) Dewar, M. J. S.; Jie, C.; Yu, G. *Tetrahedron* **1993**, *23*, 5003.
(29) Zhu, T.; Li, J.; Liotard, D. A.; Cramer, C. J.; Truhlar, D. G. *J. Chem. Phys.* **1999**, *110*, 5503.
(30) Chuang, Y.-Y.; Truhlar, D. G. *J. Am. Chem. Soc.* **1999**, *121*, 10157.
(31) Jodkowski, J. T.; Rayez, M.-T.; Rayez, J.-C.; Berces, T.; Dobe, S. *J. Phys. Chem. A* **1999**, *103*, 3750.
(32) Lendvay, G.; Berces, T.; Marta, F. *J. Phys. Chem. A* **1997**, *101*, 1588.
(33) Blowers, P.; Ford, L.; Masel, R. *J. Phys. Chem. A* **1998**, *102*, 9267.
(34) (a) Møller, C.; Plesset, M. S. *Phys. Rev.* **1934**, *46*, 618. (b) Pople, J. A.; Binkley, J.; Seeger, R. *Int. J. Quantum Chem. Symp.* **1976**, *10*, 1.
(35) Becke, A. D. *J. Chem. Phys.* **1993**, *98*, 5648. Stephens, P. J.; Devlin, F. J.; Ashvar, C. S.; Bak, K. L.; Talyor, P. R.; Frisch, M. J. *ACS Symp. Ser.* **1996**, *629*, 105.
(36) Becke, A. D. *J. Chem. Phys.* **1996**, *104*, 1040.
(37) Gordon, M. S.; Truhlar, D. G. *J. Am. Chem. Soc.* **1986**, *108*, 5412.
(38) Pople, J. A.; Head-Gordon, M.; Raghavachari, K. *J. Chem. Phys.* **1987**, *87*, 5968.
(39) Curtiss, L. A.; Redfern, P. C.; Raghavachari, K.; Rassolov, V.; Pople, J. A. *J. Chem. Phys.* **1999**, *110*, 4703.
(40) Curtiss, L. A.; Redfern, P. C.; Raghavachari, K.; Pople, J. A. *J. Chem. Phys.* **2001**, *114*, 108.
(41) Petersson, G. A.; Al-Laham, M. A. *J. Chem. Phys.* **1991**, *94*, 6081.
(42) Ochterski, J. W.; Petersson, G. A.; Montgomery, J. A., Jr. *J. Chem. Phys.* **1996**, *104*, 2598.
(43) (a) Montgomery, J. A., Jr.; Frisch, M. J.; Ochterski, J. W.; Petersson, G. A. *J. Chem. Phys.* **1999**, *110*, 2822. (b) Montgomery, J. A., Jr.; Frisch, M. J.; Ochterski, J. W.; Petersson, G. A. *J. Chem. Phys.* **2000**, *112*, 6532.
(44) Curtiss, L. A.; Raghavachari, K.; Redfern, P. C.; Rassolov, V.; Pople, J. A. *J. Chem. Phys.* **1998**, *109*, 7764.
(45) Easton, R. E.; Giesen, D. J.; Welch, A.; Cramer, C. J.; Truhlar, D. G. *Theor. Chim. Acta* **1996**, *93*, 281.
(46) (a) Lynch, B. J.; Zhao, Y.; Truhlar, D. G. *J. Phys. Chem. A* **2003**, *107*, 1384. (b) Krishnan, R.; Binkley, J. S.; Seeger, R.; Pople, J. A. *J. Chem. Phys.* **1980**, *72*, 650.
(47) Frisch, M. J.; Trucks, G. W.; Schlegel, H. B.; Scuseria, G. E.; Robb, M. A.; Cheeseman, J. R.; Montgomery, J. A., Jr.; Vreven, T.; Kudin, K. N.; Burant, J. C.; Millam, J. M.; Iyengar, S. S.; Tomasi, J.; Barone, V.; Mennucci, B.; Cossi, M.; Scalmani, G.; Rega, N.; Petersson, G. A.; Nakatsuji, H.; Hada, M.; Ehara, M.; Toyota, K.; Fukuda, R.; Hasegawa, J.; Ishida, M.; Nakajima, T.; Honda, Y.; Kitao, O.; Nakai, H.; Klene, M.; Li, X.; Knox, J. E.; Hratchian, H. P.; Cross, J. B.; Adamo, C.; Jaramillo, J.; Gomperts, R.; Stratmann, R. E.; Yazyev, O.; Austin, A. J.; Cammi, R.; Pomelli, C.; Ochterski, J. W.; Ayala, P. Y.; Morokuma, K.; Voth, G. A.; Salvador, P.; Dannenberg, J. J.; Zakrzewski, V. G.; Dapprich, S.; Daniels, A. D.; Strain, M. C.; Farkas, O.; Malick, D. K.; Rabuck, A. D.; Raghavachari, K.; Foresman, J. B.; Ortiz, J. V.; Cui, Q.; Baboul, A. G.; Clifford, S.; Cioslowski, J.; Stefanov, B. B.; Liu, G.; Liashenko, A.; Piskorz, P.; Komaromi, I.; Martin, R. L.; Fox, D. J.; Keith, T.; Al-Laham, M. A.; Peng, C. Y.; Nanayakkara, A.; Challacombe, M.; Gill, M. P. W.; Johnson, B.; Chen, W.; Wong, M. W.; Gonzalez, C.; Pople, J. A. *GAUSSIAN03*, C.01; Gaussian, Inc.: Wallingford, CT, 2004.
(48) Zhao, Y.; Rodgers, J. M.; Lynch, B. J.; Fast, P. L.; Pu, J.; Chuang, Y.-Y.; Truhlar, D. G. *MULTILEVEL*-version 4.0/G03; University of Minnesota: Minneapolis, 2004.
(49) Fast, P. L.; Corchado, J.; Sanchez, M. L.; Truhlar, D. G. *J. Phys. Chem. A* **1999**, *103*, 3139.
(50) Werner, H.-J.; Knowles, P. J.; Amos, R. D.; Bernhardsson, A.; Berning, A.; Celani, P.; Cooper, D. L.; Deegan, M. J. O.; Dobbyn, A. J.; Eckert, F.; Hampel, C.; Hetzer, G.; Knowles, P. J.; Korona, T.; Lindh, R.; Lloyd, A. W.; McNicholas, S. J.; Manby, F. R.; Meyer, W.; Mura, M. E.; Nicklass, A.; Palmieri, P.; Pitzer, R.; Rauhut, G.; Schütz, M.; Schumann, U.; Stoll, H.; Stone, A. J.; Tarroni, R.; Thorsteinsson, T.; Werner, H.-J. *MOLPRO* 2002.6; University of Birmingham: Birmingham, AL, 2002.
(51) (a) Helgaker, T.; Klopper, W.; Koch, H.; Noga, J. *J. Chem. Phys.* **1997**, *106*, 9639. (b) Csaszar, A. G.; Allen, W. D.; Schaefer, H. F., III. *J. Chem. Phys.* **1998**, *108*, 9751.
(52) Stewart, J. J. P. *J. Comput. Chem.* **1989**, *10*, 209.
(53) Stewart, J. J. P.; Rossi, I.; Hu, W.-P.; Lynch, G. C.; Liu, Y.-P.; Chuang, Y.-Y.; Pu, J.; Li, J.; Cramer, C. J.; Fast, P. L.; Truhlar, D. G. *MOPAC*-version 5.010mn; University of Minnesota: Minneapolis, 2003.
(54) Ahlswede, B.; Jug, K. *J. Comput. Chem.* **1999**, *20*, 563.
(55) Jug, K.; Bredow, T.; Geudtner, G. *MSINDO*-version 2.6; University of Hannover: Hannover, Germany, 2003.
(56) Repasky, M. P.; Chandrasekhar, J.; Jorgensen, W. L. *J. Comput. Chem.* **2002**, *23*, 1601.
(57) See http://zarbi.chem.yale.edu/utils/pddg/pddg.html.
(58) Pople, J. A.; Santry, D. P.; Segal, G. A. *J. Chem. Phys.* **1965**, *43*, S129.
(59) Pople, J. A.; Beveridge, D. L.; Dobosh, P. A. *J. Chem. Phys.* **1967**, *47*, 2026.
(60) (a) Lynch, B. J.; Truhlar, D. G. *ACS Symp. Ser.*, in press. (b) Lynch, B. J.; Truhlar, D. G. *J. Phys. Chem. A* **2003**, *107*, 8996. (c) Dybala-Defratyka, A.; Paneth, P.; Pu, J.; Truhlar, D. G. *J. Phys. Chem. A* **2004**, *108*, 2475.
(61) Martin, J. M. L.; de Oliveira, G. *J. Chem. Phys.* **1999**, *111*, 1843. Parthiban, S.; Martin, J. M. L. *J. Chem. Phys.* **2001**, *114*, 6014.
(62) Bauschlicher, C. W., Jr.; Langhoff, S. R.; Walch, S. P. *J. Chem. Phys.* **1992**, *96*, 450. Bauschlicher, C. W., Jr.; Langhoff, S. R. *Chem. Phys. Lett.* **1990**, *173*, 367.
(63) Kolos, W.; Wolniewicz, L. *J. Chem. Phys.* **1964**, *41*, 3663.
(64) Coote, M. L. *J. Phys. Chem. A* **2004**, *108*, 3865.
(65) Gonzàlez-Lafont, A.; Truong, T. N.; Truhlar, D. G. *J. Phys. Chem.* **1991**, *95*, 4618.
(66) Becke, A. D. *J. Chem. Phys.* **1996**, *104*, 1040.